



**HAL**  
open science

## Fibroblasts transfection by electroporation in 3D reconstructed human dermal tissue

Géraldine Albérola, Elisabeth Bellard, Jelena Kolosnjaj-Tabi, Jorgan Guard,  
Muriel Golzio, Marie-Pierre Rols

► **To cite this version:**

Géraldine Albérola, Elisabeth Bellard, Jelena Kolosnjaj-Tabi, Jorgan Guard, Muriel Golzio, et al..  
Fibroblasts transfection by electroporation in 3D reconstructed human dermal tissue. *Bioelectro-*  
*chemistry*, 2024, pp.108670. 10.1016/j.bioelechem.2024.108670 . hal-04459793

**HAL Id: hal-04459793**

**<https://hal.science/hal-04459793>**

Submitted on 15 Feb 2024

**HAL** is a multi-disciplinary open access archive for the deposit and dissemination of scientific research documents, whether they are published or not. The documents may come from teaching and research institutions in France or abroad, or from public or private research centers.

L'archive ouverte pluridisciplinaire **HAL**, est destinée au dépôt et à la diffusion de documents scientifiques de niveau recherche, publiés ou non, émanant des établissements d'enseignement et de recherche français ou étrangers, des laboratoires publics ou privés.



Distributed under a Creative Commons Attribution - NonCommercial - NoDerivatives 4.0  
International License



## Fibroblasts transfection by electroporation in 3D reconstructed human dermal tissue

Géraldine Albérola<sup>a,\*</sup>, Elisabeth Bellard<sup>a</sup>, Jelena Kolosnjaj-Tabi<sup>a</sup>, Jorgan Guard<sup>a</sup>, Muriel Golzio<sup>a,\*</sup>, Marie-Pierre Rols<sup>a,\*</sup>

<sup>a</sup> Institut de Pharmacologie et de Biologie Structurale (IPBS), Université de Toulouse, CNRS, Université Toulouse III - Paul Sabatier (UT3), Toulouse, France

### ARTICLE INFO

#### Keywords:

Transfection  
Electroporation  
Fibroblast  
Collagen  
Human dermal tissue  
Electrophoretic force

### ABSTRACT

The understanding of the mechanisms involved in DNA electrotransfer in human skin remains modest and limits the clinical development of various biomedical applications, such as DNA vaccination. To elucidate some mechanisms of DNA transfer in the skin following electroporation, we created a model of the dermis using a tissue engineering approach. This model allowed us to study the electrotransfection of fibroblasts in a three-dimensional environment that included multiple layers of fibroblasts as well as the self-secreted collagen matrix. With the aim of improving transfection yield, we applied electrical pulses with electric field lines perpendicular to the reconstructed model tissue. Our results indicate that the fibroblasts of the reconstructed skin tissue can be efficiently permeabilized by applied millisecond electrical pulses. However, despite efficient permeabilization, the transfected cells remain localized only on the surface of the microtissue, to which the plasmid was deposited. Second harmonic generation microscopy revealed the extensive extracellular collagen matrix around the fibroblasts, which might have affected the mobility of the plasmid into deeper layers of the skin tissue model. Our results show that the used skin tissue model reproduces the structural barriers that might be responsible for the limited gene electrotransfer in the skin.

### 1. Introduction

The development of non-viral methods for nucleic acids delivery has gained exciting and increasing interest these last few years due to the translation of such methods to the clinics with COVID-19 vaccines. Since December 2019, a number of research centres and companies have raced to develop vaccines, including conventional viral and protein-based jabs, as well as DNA- and mRNA-based vaccines [1]. Lipid nanoparticles were used to deliver mRNA [2]. Beside nanovectors, other non-viral methods such as electroporation have shown promising results for gene transfer, including but not limited to mRNA. To be used in the clinic, gene transfer methods must be both safe and efficient. These criteria are fully met by electroporation. Electroporation is a physical method for molecules delivery based on the local application of pulsed electric fields to cells and tissues. Above a certain threshold, the electric field leads to the permeabilization of cell membranes. This phenomenon, the “electropermeabilization”, is also known under the term “electroporation”, due to its simplest description as the formation of pores within the cell membrane. Depending on the parameters of

electric pulses (namely the electric field intensity, pulses number and duration), the permeabilization of the cells can be transient (reversible) or irreversible, and can be used to transfer molecules of different sizes and charges into cells and tissues. The excellent efficacy, safety and convenient mouldability of electroporation parameters led to the development of electroporation-based technologies and their translation from laboratories to clinic, mainly for cancer therapies, but also for cell and gene therapies [3]. Reversible electroporation has been developed as a method, which improves anti-tumor response induced by chemotherapy (the technique combining the application of pulsed electric field with chemotherapy is called electrochemotherapy). This strategy allows to dramatically increase the penetration of non-permeant or poorly permeant drugs into cancer cells due to the transient formation of small pores in the cell membrane. In 1991, Mir et al. conducted an early phase clinical trial and demonstrated that bleomycin can be efficiently introduced into malignant cells in humans with cancer, highly and locally potentiating the effect of the mentioned cytotoxic drug [4]. In 2005, Davalos et al. showed that irreversible electropermeabilization induces cancer cells death with minimal heating effects (a technique called

\* Corresponding authors.

E-mail addresses: [Muriel.Golzio@ipbs.fr](mailto:Muriel.Golzio@ipbs.fr) (M. Golzio), [Marie-Pierre.Rols@ipbs.fr](mailto:Marie-Pierre.Rols@ipbs.fr) (M.-P. Rols).

<https://doi.org/10.1016/j.bioelechem.2024.108670>

Received 27 November 2023; Received in revised form 31 January 2024; Accepted 12 February 2024

Available online 13 February 2024

1567-5394/© 2024 The Authors. Published by Elsevier B.V. This is an open access article under the CC BY license (<http://creativecommons.org/licenses/by/4.0/>).

irreversible electroporation) [5]. In this procedure, both the tissue extracellular matrix, the vessels collagen structures and nerves architectures are preserved, allowing the regeneration of tissues. The approach is unique, safe and therefore differs from thermal ablative techniques.

Another expanding field relying on electroporation concerns gene electrotransfer. In 1982, Neumann et al. published the first electroporation-mediated gene transfer experiment in cells [6]. Since then, the translation to clinics took advantage of the increasing knowledge of mechanisms involved in the electrotransfer of nucleic acids [7–9]. In 2002, Golzio et al. showed that the transfer of genes into cells is much more complex than the transfer of small molecules. The process involves both the electropermeabilization of the cell membrane and the electrophoresis of plasmid DNA towards the electropermeabilized membrane, where plasmid DNA first forms complexes with cell membranes during pulses application, and subsequently enters the cells in the minutes following pulses application. The first evidence for gene electrotransfer in murine tumors was reported by Rols et al. in 1998 [10]. In 2008, Daud et al. reported the first clinical trial in patients with metastatic melanoma [11].

Gene electrotransfer can nowadays be performed in almost all tissues including the skin. In 1981, Titomirov et al. [12] were the first to report that skin cells of new-born mice could be stably transformed *in vivo* using electroporation. Expression was detected in fibroblast extracted from the dermis. Overall, skin electroporation appears as a promising technology for a number of applications including transdermal drug delivery, electrochemotherapy and wound disinfection in addition to gene electrotransfer [13]. The intradermal injection of DNA followed by the skin permeabilization with electric pulses produces a local treatment depending on the spatial and temporal distribution of the DNA and the electric field.

This technology has the main advantages of being easy to use, fast, reproducible and safe. However, despite a considerable number of *in vitro* and *in vivo* studies, with promising results for wound healing [14] and vaccination [15], translation to clinics is not as fast as one would expect, due to inadequate protocols and dosimetry (electrode configurations, pulse parameters) and differences in animal and human skin [13]. Different electrodes configurations have been developed, from non-invasive contact electrodes [16] to multi-electrode arrays [17], and different pulse parameters were used employing various electric field intensities and pulse durations. Using contact electrodes, the combination of short high voltage pulses and long medium voltage pulses allowed to obtain a high expression of both reporter and therapeutic genes in safe protocols applied to living animals [18,19]. Beside the electrophoretic contribution of the electric field for nucleic transfer in cells [20,21], the orientation of the electric field can also increase the biodistribution of these charged molecules in tissues such as muscle [22,23].

Nevertheless, when compared to viral or lipid-nanoparticle mediated transfection, the transfection yield following electroporation lags behind. Mechanistic studies are thus still required in order to understand and overcome the barriers, responsible for poor DNA migration towards cells, which present the first step for successful gene electrotransfer. One of the main causes of low *in vivo* electrotransfer efficiency is the relatively low mobility of DNA in tissues compared to the mobility within *in vitro* conditions [24].

In order to closely evaluate the effect of the native (cell-secreted collagen matrix) in gene electrotransfer processes, relevant biological models of human dermal tissue have been developed. The tissue engineering self-assembly approach [25] allows to produce reconstructed human dermal tissue, rich in native extracellular matrix [26]. Primary human dermal fibroblasts reproduce a native environment by secreting and organizing a 3D extracellular matrix rich in collagens. These abundant collagen fibrils can be detected by second harmonic generation [27]. In previous studies, we showed that such 3D cell tissue-engineered model can be electropermeabilized and transfected with

millisecond electric pulses using contact electrodes [27,28]. In that case, the contact electrodes were placed on the top of the cell sheet, therefore the electric field was applied parallel to fibroblasts layers. Under such experimental conditions [27,28], only the cells present in the outer layer of the cell sheet were transfected.

In the quest for transfection of deeper cell layers in dermal cell sheets, the aim of this study was to evaluate and improve gene electrotransfer in this relevant and useful biological model. We thus studied the effects of the electric field pulses using a different electrode design in comparison to previous studies [27,28]. With such electrodes we were able to deliver the pulses perpendicularly across the thickness of the cell sheet. Moreover, we evaluated the application of extended pulses duration (5 and 20 ms), to potentially improve the transfection by amplifying the duration of electrophoretic drag and thus potentially attaining deeper layers of the sheet.

## 2. Materials and methods

### 2.1. Cell culture

Primary human dermal fibroblasts were isolated from a 3-year-old child's foreskin purchased from Icelltis (Toulouse, France) as previously described [28]. Primary cells were grown in 5 % CO<sub>2</sub> humidified atmosphere at 37 °C in Dulbecco's Modified Eagles Medium (Gibco-Invitrogen, Carlsbad, USA) supplemented with 10 % heat-inactivated foetal calf serum, 100 U/mL penicillin and 100 µg/mL streptomycin. Cells were exposed to pulsed electric field either in suspension (see [Supporting information](#)) or in 3D engineered tissues (described in the following text).

### 2.2. Reconstruction of human 3D engineered dermal tissue

Human dermal substitutes are engineered dermal tissues or “cell sheets”, consisting of primary dermal fibroblasts, embedded in their self-secreted extracellular matrix. The structures do not contain any exogenously added extracellular matrix material. Cell sheets were created *in vitro* according to the self-assembly approach. Thirty thousand primary human dermal fibroblasts were seeded and grown in Whatman filter paper anchoring ring (inner diameter 10 mm, outer diameter 15 mm)-containing 24-well plates, over a period of four weeks in cell culture medium supplemented with 50 µg /mL of ascorbic acid (Sigma Aldrich USA) as previously reported [28]. After four weeks, the cell sheets contain a dense extracellular matrix, which allows the manipulation of the 3D structure, as the dermal sheet is thick enough (with average thickness of 50 +/- 10 µm) and remains attached to the anchoring paper, which can be manipulated with tweezers. Since cell sheets consist of primary dermal fibroblasts, their extracellular matrix is comparable to the one of human dermis, as we previously showed [29].

### 2.3. Electropermeabilization and gene electrotransfer

Cell sheets were immersed in pulsing buffer (also known as ‘ZAP’, containing 8.1 mM dipotassium phosphate, 1.9 mM monopotassium phosphate, 1 mM magnesium chloride in water and 250 mM sucrose), placed between two parallel electrode plates. To assess cell permeabilization, the cell sheet was placed in 600 µL of ZAP buffer containing 100 µM of propidium iodide (PI) (Sigma Aldrich, USA) and analysed 20 min after pulse application [27,28]. For gene electrotransfer, 1.6 µL of plasmid solution containing 4 µg of tdTomato DNA plasmid (Invivogen, Toulouse, France) were placed on the top of the cell sheet lying between two parallel plate electrodes in ZAP buffer, as shown in [Fig. 1](#). The positive electrode was set on the bottom of the cell sheet. Using this set-up, the electrophoretic drag should push the DNA through the cell sheet. Electropulsation was performed with an ELECTRO cell S20 generator (βTech, Toulouse, France), which delivered square wave electric pulses. Pulse parameters were as follows: 8 pulses

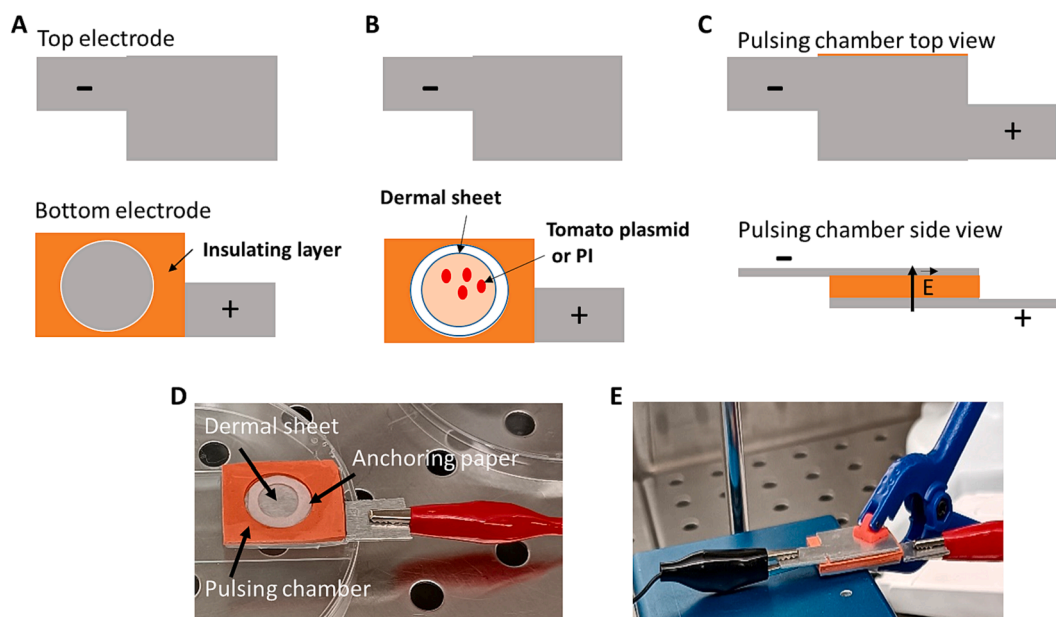


**Fig. 1.** Experimental pulsing chamber. A- Schematic representation of the components of the used electrode device. Graphic representation of two parallel planar stainless-steel electrodes with the negative electrode at the top and the positive electrode at the bottom. An insulating silicone sheet spacer is placed between the electrodes to delimit the reservoir of the pulsing chamber. B- Positioning of the dermal sheet, attached to the anchoring paper (white ring), in the pulsing chamber containing ZAP buffer supplemented with PI (100  $\mu\text{M}$ ) for electropermeabilization experiments. For gene electrotransfer, 4  $\mu\text{g}$  of tdTomato DNA plasmid were placed on the upper surface of the dermal sheet. C- Closed pulsing chamber. D- Photograph of the open device with the dermal sheet inside the pulsing chamber. E- Closed electroporation system.

lasting 5 or 20 ms, delivered with a pulse repetition rate of 1 Hz using electric field intensities of 0, 400 V/cm, 600 V/cm, and 800 V/cm at room temperature. After procedure, dermal sheets were placed again in 24-well plates.

Cell electrotransfer of fibroblasts in suspension is described in [Supporting Information](#).

#### 2.4. Cell viability assessment

Cell viability was assessed in two experimental settings, using either Hoechst staining (blue fluorescence) in presence of Tomato-expressing cells, or using PI (red fluorescence) to detect non-viable cells.

**Hoechst staining.** Hoechst 33258 (Invitrogen, #H3569) was used in order to stain dead cells 48 h after application of the electric field. Syto 16 Green Fluorescent Nucleic Acid Stain (Invitrogen#S7578) was used to stain all nuclei. Briefly, dermal sheets were incubated for 1 h at 37  $^{\circ}\text{C}$  with Syto 16 (1 mM stock solution in DMSO), in culture medium at a dilution of 1/1000. Subsequently, dermal sheets were incubated for 10 min at 37  $^{\circ}\text{C}$  in culture medium containing Hoechst 33258 (dilution 1/5000).

**Propidium iodide.** As Hoechst 33258 can underestimate cell viability [30], we also used PI for cell viability detection in a separate experiment. The method consists in the addition of 100  $\mu\text{M}$  of PI (Sigma Aldrich, USA), 24 h or 48 h after application of the electric field. The stained dermal sheets were placed directly into the imaging chamber for fluorescence imaging.

#### 2.5. Microscopy

The whole cell sheet observation of Hoechst 33258, Syto 16, Tomato and PI-positive cells was performed in a 2D projection, using an upright fluorescence widefield microscope (Macrofluor, Leica Microsystems SA, Rueil-Malmaison, France), equipped with a Cool Snap HQ2 Camera (Roper Scientific, Photometrics, Tucson, AZ, USA) using appropriate filters for all fluorophores (Hoechst 33258: excitation filter 450/50 nm; emission filter 420LP nm; Syto 16: excitation filter 480/40 nm; emission

filter 527/30 nm and for PI and tomato: excitation filter 560/40 nm, emission filter 630/75 nm). Images were acquired at different magnifications ( $\times 1.25$ ;  $\times 5$  and  $\times 25$ ) and subsequently analysed with imageJ analysis software (NIH, Bethesda, USA).

The 3D multiphoton microscopy of the cell sheet, including the in situ generated collagen, Hoechst 33258, Syto 16, Tomato and PI-positive cells was conducted using a 7MP multiphoton microscope (Carl Zeiss, Jena, Germany) equipped with a 20 $\times$  objective (NA 0.95) and coupled to a Ti-Sapphire femtosecond laser, Chameleon Ultra 2 (Coherent Inc) tuned to 760 for Hoechst 33258, 800 nm for PI and 920 nm for Tomato and Syto 16 signals. Organized fibrillar collagens were detected with both excitation wavelengths by second harmonic generation (SHG) through a 485 nm short pass filter, Syto 16 through a 500–550 band pass filter, Hoechst 33258 through a 435–485 band pass filter and PI and Tomato positive cells, through a 565–610 nm band pass filter with non-descanned detectors. For Tomato dermal sheets, 3D stacks (425 $\times$ 425  $\mu\text{m}$ , variable z) were acquired at a resolution of 0.42  $\mu\text{m}$  and with z-stacking of 1  $\mu\text{m}$ . For PI dermal sheets, mosaics (2 $\times$ 2) of 3D stacks (807 $\times$ 807  $\mu\text{m}$ , variable z) were acquired at a resolution of 0.42  $\mu\text{m}$  and with z-stacking of 2  $\mu\text{m}$ . The acquired 3D images were subsequently analysed with Imaris software (Bitplane AG).

#### 2.6. Data analysis

To quantify Hoechst 33258 and PI-positive cells area using ImageJ software, three regions of interest (ROI) of equal size were defined for each 2D micrograph. For Tomato-positive cells, one ROI was selected. Subsequently, a suitable threshold was applied to obtain a mask of the positive cells for each ROI. From this mask, the area occupied by positive cells for each ROI was determined. Positive area percentages were calculated relative to the size of the ROI.

From the 3D multiphoton micrographs, we determined both the volume of positive cells and the volume of the dermal sheet using Imaris software. To quantify PI positive cells volume, a suitable threshold was applied on PI channel to obtain a mask of PI-positive cells. The volume of the dermal sheet was determined using a suitable threshold on the SHG

channel. Volume occupancy rate of PI positive cells in percentage was calculated relative to the volume of a dermal sheet.

### 2.7. Pulse temperature measurement

To determine the thermal increment due to the delivery of electric pulses, the temperature increase was measured with the Nomad Fiber Optic Thermometer (Model NMD 535 A) probe placed in the pulsing chamber containing 600  $\mu$ L of ZAP buffer.

### 2.8. Statistical analysis

The number of biological replicates (n) (usually three different cell sheets) were studied in two or three independent experiments (N). GraphPad Prism 6 program (GraphPad Software, Inc., La Jolla, CA, USA) was used for statistical analyses. All quantifications were plotted as mean  $\pm$  standard error mean (SEM), and overall statistical significance was set at p-value  $<0.05$ . One-way ANOVA with Bonferroni's multiple comparison test or t-tests were performed.

## 3. Results and discussion

We have previously shown that fibroblasts containing engineered dermal sheets can be transfected by electroporation, when the electric field is applied parallel to the dermal sheet [28]. As in the previous setting the electric field was not homogenous over the entire thickness of the sheet, and as the transfection was limited to the upper layer of the sheet, we herein investigated a different electrode setting, in which the electric field is applied perpendicularly to the dermal sheet.

We applied "standard" electrical parameters for gene electrotransfer, which were the same as the ones used in our previous study made with

contact electrodes [28]. In addition, we herein also applied electric pulses with a longer pulse duration (20 ms), which showed promise in a previous work performed on mice skin [31], where electrophoresis was shown as the main driving force for macromolecules transdermal delivery.

We used two imaging modalities to visualize and quantify the effect of pulse parameters on cell permeabilization, gene transfection and to assess cell viability in native (unfixed) human cell sheets. First, fluorescence macroscopy imaging allowed the visualization of the efficiency of cell sheet permeabilization and gene electrotransfection. In addition, the viability was assessed at the tissue scale via cellular uptake of Hoechst 33258 (in combination with tomato transfection) or by PI uptake alone. Subsequently, multiphoton microscopy allowed the visualization of the cells in 3D within the tissue, allowing the precise location of transfected cells and enabling the visualization of dead cells within the collagen-containing tissue in native and electroporated tissues. Altogether, these methodologies allowed us to address the effect of pulse parameters and electric field direction on gene transfection efficiency in dermal sheet fibroblasts, determine a precise location of the transfected cells in 3D and assess the impact of electric pulses on cell viability.

### 3.1. Effect of electric field strength and pulse duration on cell permeabilization

A prerequisite for plasmid delivery is cell membrane permeabilization. In order to determine if cells within the dermal sheet can be efficiently permeabilized or whether cell permeabilization could differ in different zones of cell sheets, we evaluated cell permeabilization upon exposure to different pulse parameters. The 3D reconstructed dermal model was submitted to electrical pulses in ZAP buffer containing 100  $\mu$ M PI (Fig. 2). When added during electropulsation, PI revealed some

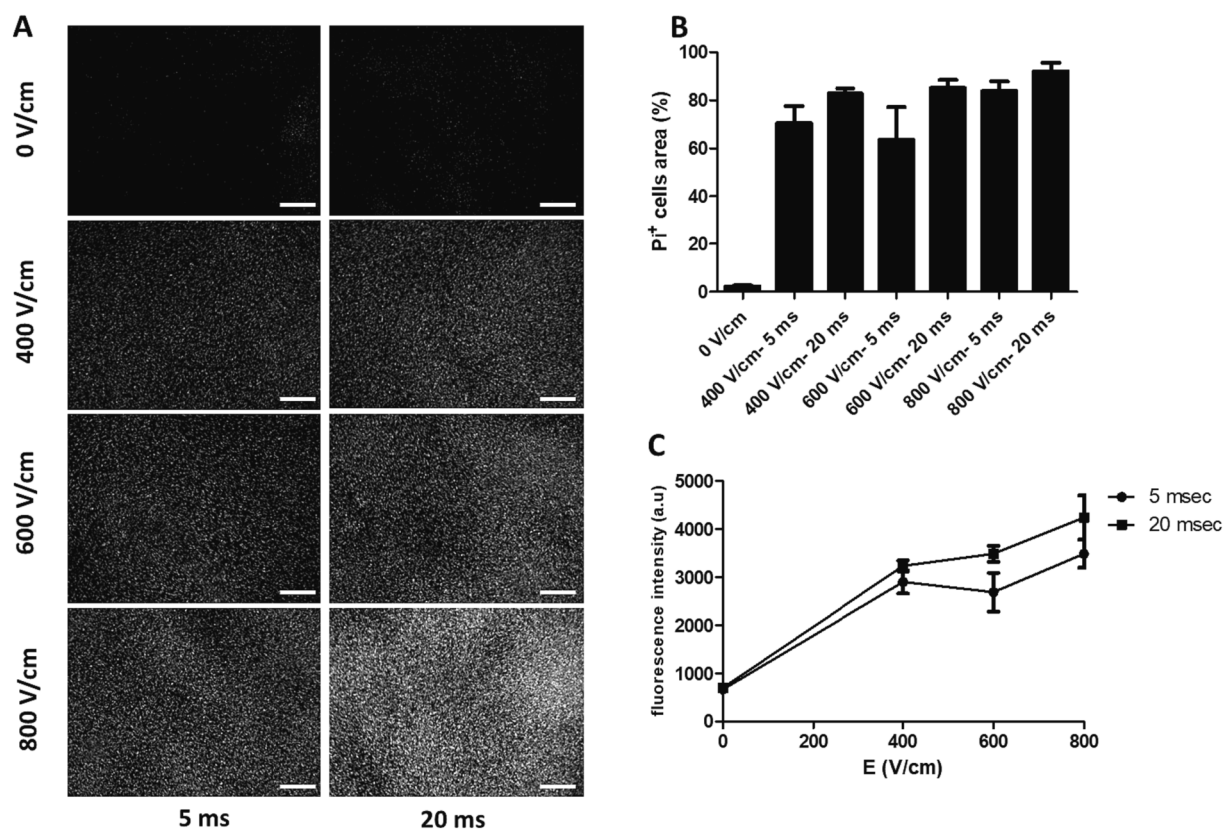


**Fig. 2.** Effect of electric field strength and pulse duration on cell permeabilization. Cell permeabilization within tissues following the application of electric pulses, showing propidium iodide (PI) incorporation within permeable cells. A- Representative fluorescence images of PI labelling (white) in the 3D dermal sheet 20 min post-pulse exposed to different parameters, as evidenced by fluorescence macroscopy. Scale bar: 0.5 mm. B- PI positive cells areas and C associated fluorescence intensities were quantified on the macro-fluo images of the tissue using ImageJ software (N = 2, n = 6).

scattered constitutive dead cells (present because of the natural turnover of 3D-grown dermal fibroblasts) and cells that have been permeabilized upon application of the electric field (Fig. 2A). Quantification of images showed that the percentage of PI-positive cells was high and homogeneous at 400 V/cm and slightly increased with the increase of the electric field intensity (Fig. 2B). The quantification of the fluorescence intensity showed that pulses with 20 ms duration slightly increased the amount of PI entering the permeable cells (Fig. 2C), in comparison to 5 ms pulses.

### 3.2. Effect of electric field strength and pulse duration on gene transfection efficiency and cell viability

The 3D reconstructed dermal model was submitted to electrical pulses in presence of 4  $\mu$ g of tdTomato reporter plasmid (Fig. 3A). Tomato expression was observed by fluorescence macroscopy imaging 48 h after plasmid electrotransfer. No transfected cells were detected in absence of electric field (upper pair of panels in Fig. 3A) or absence of plasmid DNA (figure not shown). The observation of cell sheets showed that the 4 conditions (5 ms and 20 ms pulses) with electric field intensity

of 400 and 600 V/cm led to cell transfection. Transfection of some cells, constituting the dermal sheet, was observed at 400 V/cm for both pulses duration protocols, 5 and 20 ms (Fig. 3A, second pair of panels). The quantification of Tomato-positive area 48 h after plasmid exposure revealed that the most efficient electric field pulses parameters were 400 V/cm with pulses duration of 20 ms. Yet, the number of Tomato-expressing cells did not increase with the electric field intensity (Fig. 3A, third and fourth pair of panels). Precisely, the transfection rates even decreased at field intensities of 600 V/cm and 800 V/cm (Fig. 3B). A possible reason could be related to a decreased viability of cells under these exposure conditions.

To address the assumption that viability might be affected, we also stained dermal sheets with Hoechst 33258 48 h after pulse (Fig. 4A). Nevertheless, the results obtained at 800 V/cm (bottom pair of panels in Fig. 4A) appeared incoherent, we thus performed an additional viability assessment with propidium iodide uptake 24 h after pulse (Fig. 4D and E).

Membrane resealing and repair usually occurs within about 20 min after the application of millisecond pulses [32]. Thus, when Hoechst

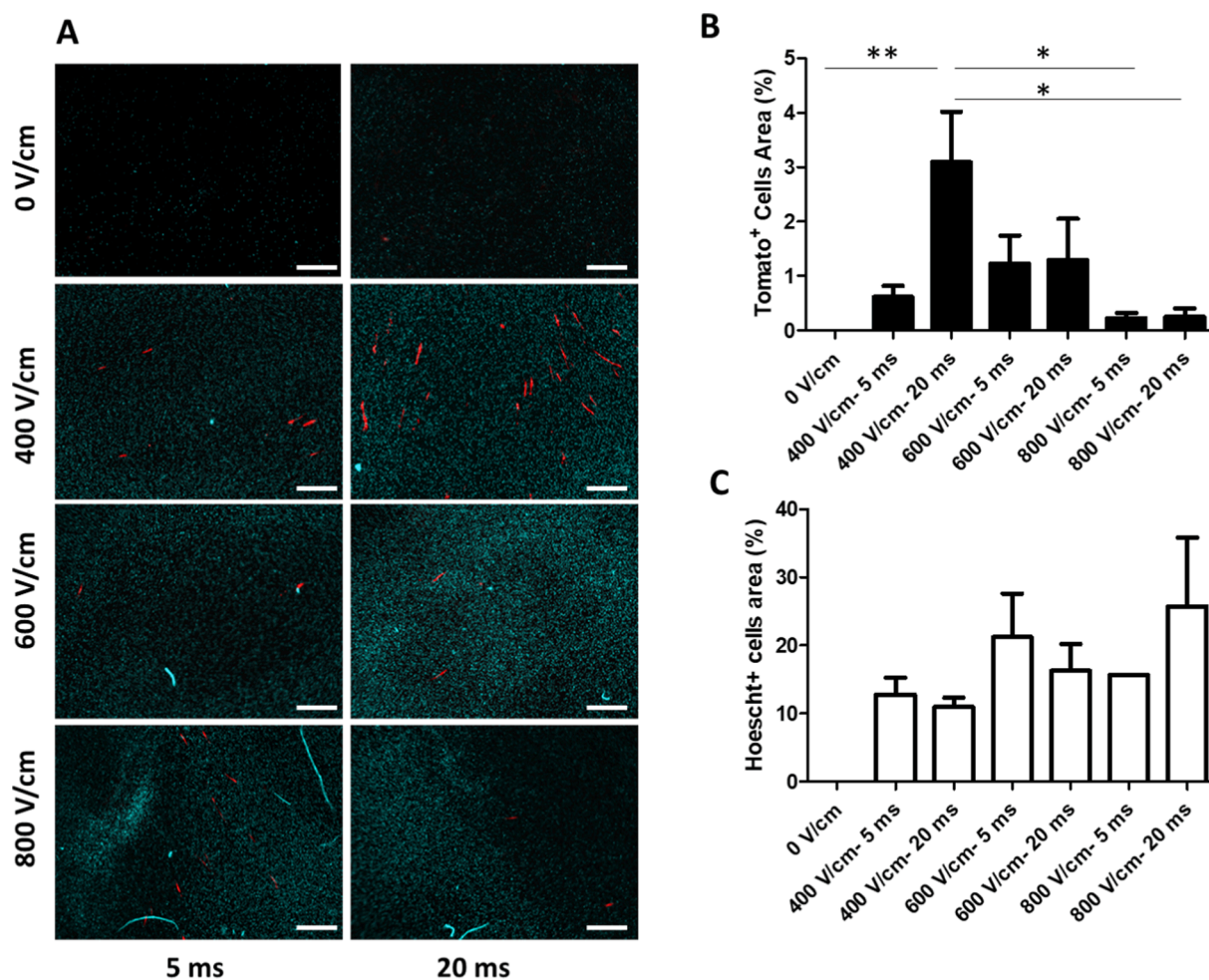


**Fig. 3.** Effect of the electric field strength and the pulse duration on gene transfection efficiency and on cell viability. Tomato expression in 3D cell sheets was observed by macroscopy 48 h after plasmid exposure. A- Representative micrographs of Tomato expression (red) counterstained with Hoechst 33258 (cyan) for cell viability in selected central zones of 3D dermal sheets submitted to different electric field intensities and different pulse durations. Scale bar: 1 mm. B - Quantification of Tomato-positive area in percentage (%) corresponding to the surface of the fluorescently electrotransfected cells relative to the total surface observed on macrofluor images of dermal sheets. One-way ANOVA, \*\*  $p < 0.01$ ; \*  $p < 0.05$ ;  $N = 2$  independent experiments with  $n = 6$  dermal sheet per experiment..C- Quantification of Hoechst-positive area in % corresponding to the surface of dead cells, there was no significant difference ( $p$ -value  $> 0.05$ ). D- PI labelling (white) on the 3D dermal sheet 24 h post-pulse with different parameters (0–400–600–800 V/cm with 5 or 20 ms pulse duration) evidenced by fluorescence macroscopy (red-square inset shows the magnified zone), scale bar: 0.5 mm. Zoom 5X (red square) of the condition 800 V/cm with 20 ms pulse duration showing positive PI cells in detail. B- PI positive cells area quantified on the macrofluor images of the tissue using Image J software. One-way ANOVA, \*\*\*\*  $p < 0.0001$ , \*\*\*  $p < 0.001$ ; \*  $p < 0.05$ ;  $N = 2$  independent experiments with  $n = 6$  dermal sheet per experiment. (For interpretation of the references to color in this figure legend, the reader is referred to the web version of this article.)

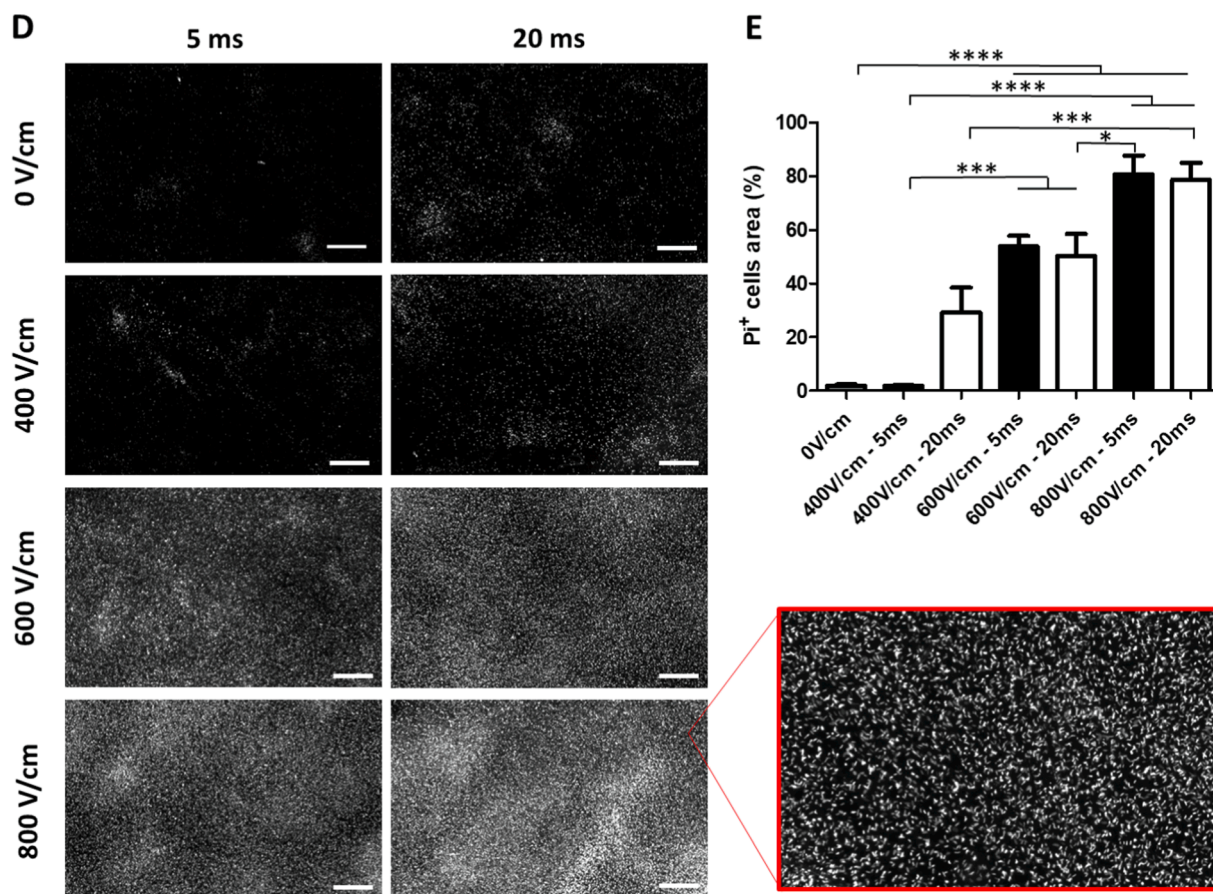


Fig. 3. (continued).

33258 was added at 48 h after electropulsation, the dye only enters into dead cells, which can either correspond to the fraction of dead cells, which died due to the natural cell turnover in the dermal sheet (also termed constitutive dead cells), or to the fraction of cells, which were irreversibly permeabilized by electric pulses.

As Hoechst 33258 could underestimate the cell viability [30], which was also our assumption following the observation of dermal sheets exposed to 800 V/cm conditions (Fig. 3A bottom pair of panels), PI was added 24 h after the application of electric pulses in absence of DNA. The results (Fig. 3D and E) confirmed that PI allowed a more sensitive labelling, evidencing cell mortality at electric field intensity of 800 V/cm. We thus confirmed that the increase of electric field intensities correlates with increased cell mortality.

Altogether, the results on cell permeabilization (Fig. 2) and cell viability (Fig. 3) substantiate the observation that at 600 V/cm and 800 V/cm there were less or few transfected cells, because irreversible permeabilization compromised the viability of the cells at higher intensity electric pulses, and thus the cells were unable to express the applied plasmid. The 400 V/cm condition had little effect on cell viability and therefore resulted in better gene expression. Although informative about the effect of the electric field strength and pulse duration on cell transfection and cell viability, at the tissue scale, these observations did not allow to determine if any transfected cells were located in the depths of dermal sheets. Therefore, these data did not provide evidence related to the benefit of the perpendicular orientation of the electric field on the transfection of deeper cell layers embedded within the dermal sheet.

### 3.3. Localization of the permeabilized and viable fibroblasts in 3D

The analysis of dermal sheets by multiphoton microscopy allows the localization of the permeabilized cells in presence of PI on 3D stacks.

Cross-sectional views (top and transversal views) showed that at 0 V/cm, some dead cells could be visualized. These PI labeled cells correspond to dead cells that were mainly located in the lower part of the dermal-sheet (Fig. 4A). This is consistent with the presence of a gradient of proliferating cells from the bottom to the top (with proliferative cells located on the top). Subsequently, increasing the electric field strength resulted in an increase of “permeabilized” cells along the thickness of the dermal sheet (Fig. 4A). This observation indicates that the current efficiently passed through the different layers of the sheet and that electroporation occurred in the entire tissue. Moreover, as indicated by concomitant Hoechst 33258 and Tomato staining (Fig. 3A), increasing the pulse duration time improved red protein expression at 400 V/cm, but cell viability slightly decreased (Fig. 3D). When the intensity was increased to 600 or 800 V/cm, the viability was considerably altered and red protein expression was not improved in comparison to the conditions where cells were exposed to 400 V/cm (Fig. 3).

This loss of cell viability with the increase of the electric field strength was clearly observed using PI labelling 24 h after pulse application (Fig. 4B). Quantification of the volume corresponding to the occupancy of PI positive cells in percent showed the weakest effect on cell viability for the 400 V/cm condition.

### 3.4. Effect of the field orientation and direction on the localization of the transfected fibroblasts

The analysis of transfected sheets by multiphoton microscopy allows the localisation of transfected cells in dermal reconstructs. Cross-sectional views (top and transversal views) showed that only the cells present at the top of the cell sheet were transfected, regardless of the electric field intensity and pulse duration (Fig. 5A and B). This could be due to many factors: (i) living or metabolically active and therefore

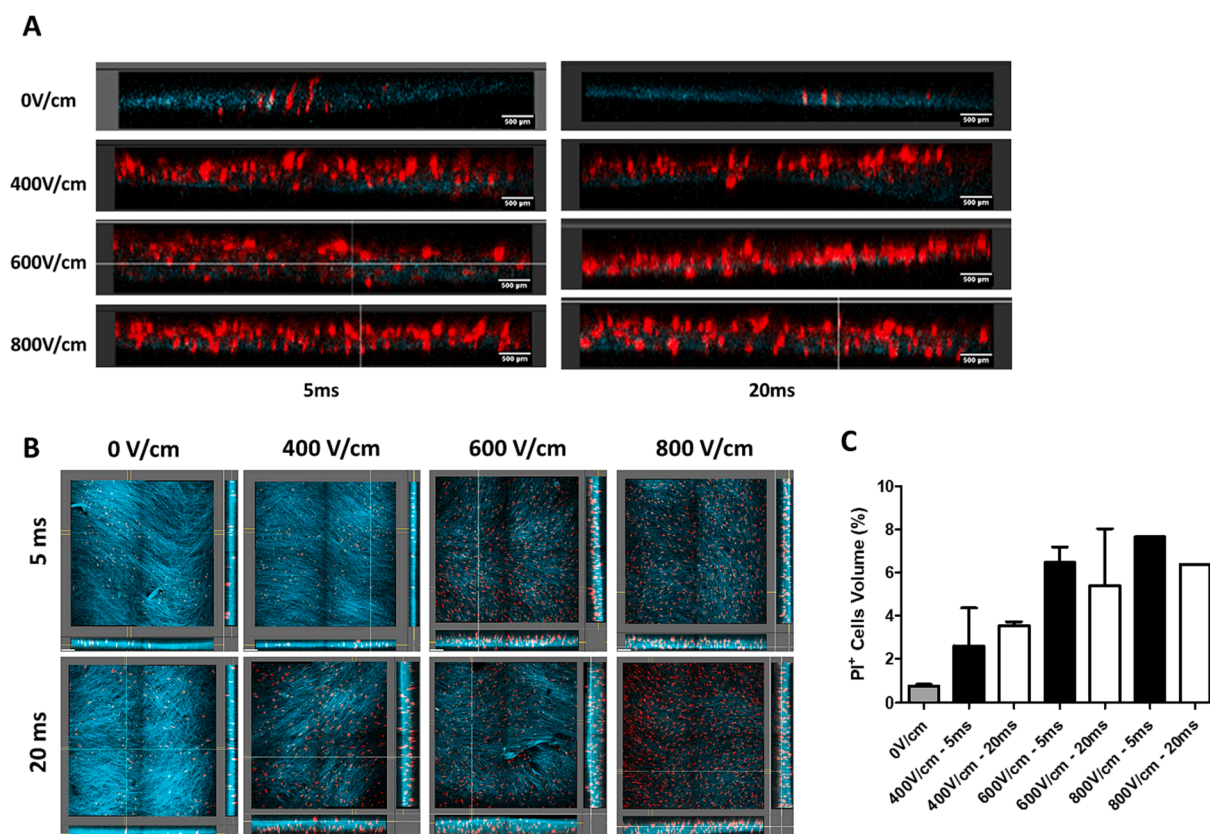


**Fig. 4.** Localization of permeabilized and dead fibroblasts in 3D dermal sheets by multiphoton microscopy detection. A and B - Second harmonic generation micrographs with orthogonal view showing PI positive cells in the dermal sheet after electroporation with different pulse parameters (0–400–600–800 V/cm with 5 or 20-millisecond pulse durations) evidencing (A) the localisation of permeabilized cells; (B) the localisation of dead cells at 24 h. Scale bar: 150  $\mu\text{m}$ . C- quantification of dead PI-positive cells volume. (N = 1; n = 2).

transfected cells, only present on the upper surface, ii) presence of the collagen in deeper layers, preventing DNA migration to deeper layers of the cell sheet, iii) a compromised electrophoretic force, which is too low to push plasmid DNA towards the electroporeabilized cell membranes, located in the lower layers.

Even if the electroporeabilization is mandatory, it is not a sufficient condition for gene transfection. In our previous work, we evaluated the proliferative cells using an enzymatic assay and estimated that cells were homogeneously distributed through the 3 dimensions within the reconstructed dermal tissue as no differences were observed between transfected and control dermal sheet [28]. Here, using 3D acquisition, we observed more dead cells at the bottom of the dermal sheet suggesting the presence of a cell proliferation gradient. Thus, a potential explanation for transfected cells occurring only at the surface of the cell sheet, is that only these cells are proliferative, while bottom cells are quiescent. Proliferative cells are usually more efficiently electroporeabilized, due to the disintegration of the nuclear envelope during mitosis, enhancing gene expression due to the direct access of DNA plasmid to the nucleus [33].

To test this hypothesis, we subsequently decided to flip the dermal sheet and apply the plasmid on the other side of the dermal sheet, to test if viable cells from the lowest layer could be transfected. When plasmid DNA was added on the non-proliferating side of the dermal sheet (Fig. 6), macroscopic acquisitions of tomato expressing cells showed that the percentage of transfected cells was significantly lower compared to the previous experiment (Fig. 6A, 6B and 6E). The 3D analysis following biphoton microscopy in Fig. 6C and 6D, showed that: 1) as expected, there were a few dead cells (blue labelling) and all the tomato positive cells were viable as they displayed green fluorescence in the nucleus; 2) cell expressing tomato were again only located on the side of tissue

where the plasmid DNA was deposited. Being less proliferative, cells from the lowest side of the cultured dermal sheet could be less prone to transfection, in agreement with previous studies reporting that the transfection is more efficient in proliferative cells [34]; 3) the expression was located on the bottom side of the dermal sheet, beyond the collagen, where the plasmid was deposited. Therefore, we could conclude that the plasmid DNA was not able to cross the dermal sheet.

Another explanation for decreased transfection could come from the fact that the reconstructed human dermal tissue is rich in collagens and therefore that DNA plasmid electrophoretic transport is hindered by the collagen as shown in tumor tissue [35].

In order to determine the degree of transfection in collagen free conditions, suspended fibroblasts were exposed to electric pulses, with parallel electrodes (Leroy Biotech, France), as described in Supporting Information. As expected, in such setting, the transfection was considerably more efficient than in 3D (Supporting Fig. 2), with the transfected cells fraction reaching more than 30 % of the cell population, which is considerably more than the couple of transfected cells observed in the 3D model. This experiment confirmed that fibroblasts alone can be more easily transfected in a barrier-free and proliferative configuration.

Collagen is a structural component that profoundly affects the therapeutic outcome in solid tumors [36]. Precisely, the collagen can prevent the penetration of systemically administered anticancer agents into the tumor core [37]. Nevertheless, when tumor tissue is mildly heated (to about 40 °C), the collagen network is altered, and therapeutic agents (such as doxorubicin [37]) can protrude into the tumor. Mild thermal treatments of the collagen matrix could thus improve the penetration of therapeutic agents.

In electroporation settings the scientific and medical community generally stem to reduce thermal effects, because if they are excessively



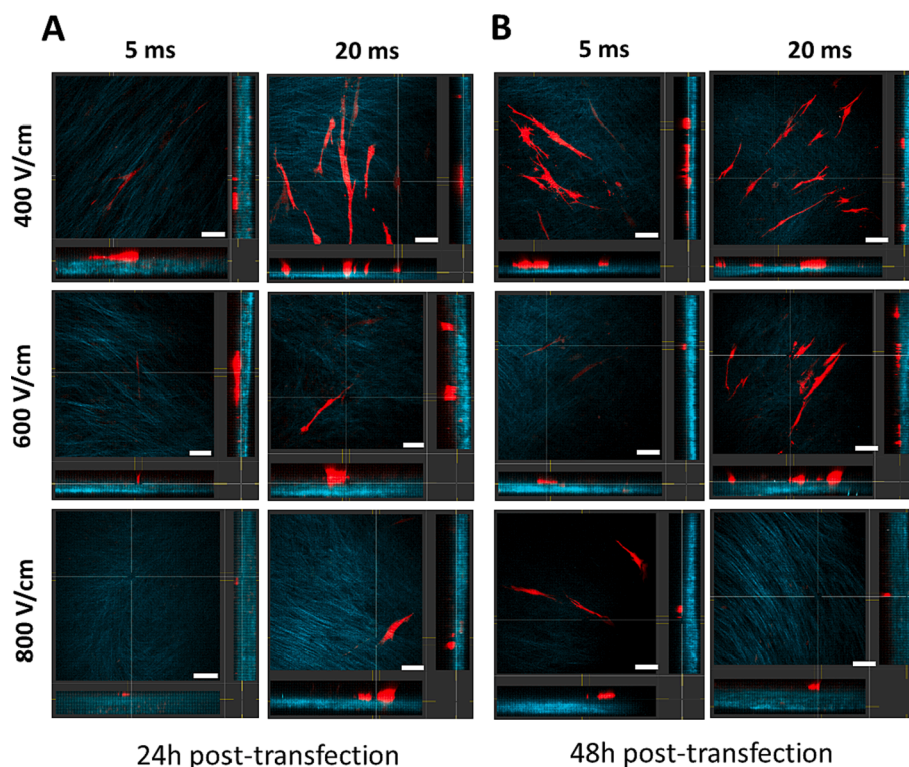


**Fig. 5.** Localization of the transfected fibroblast in 3D dermal sheets by multiphoton detection. Representative second-harmonic generation (SGH) micrographs with orthogonal view showing Tomato expressing cells (red) located on the upper surface, above the collagen fibres (SHG- blue) following the application of different parameters (400–600–800 V/cm with 5 or 20 ms pulsation duration) after 24 h (A) and 48 h (B) following electrotransfection. Scale bar: 150  $\mu$ m. (N = 2; n = 6). (For interpretation of the references to color in this figure legend, the reader is referred to the web version of this article.)

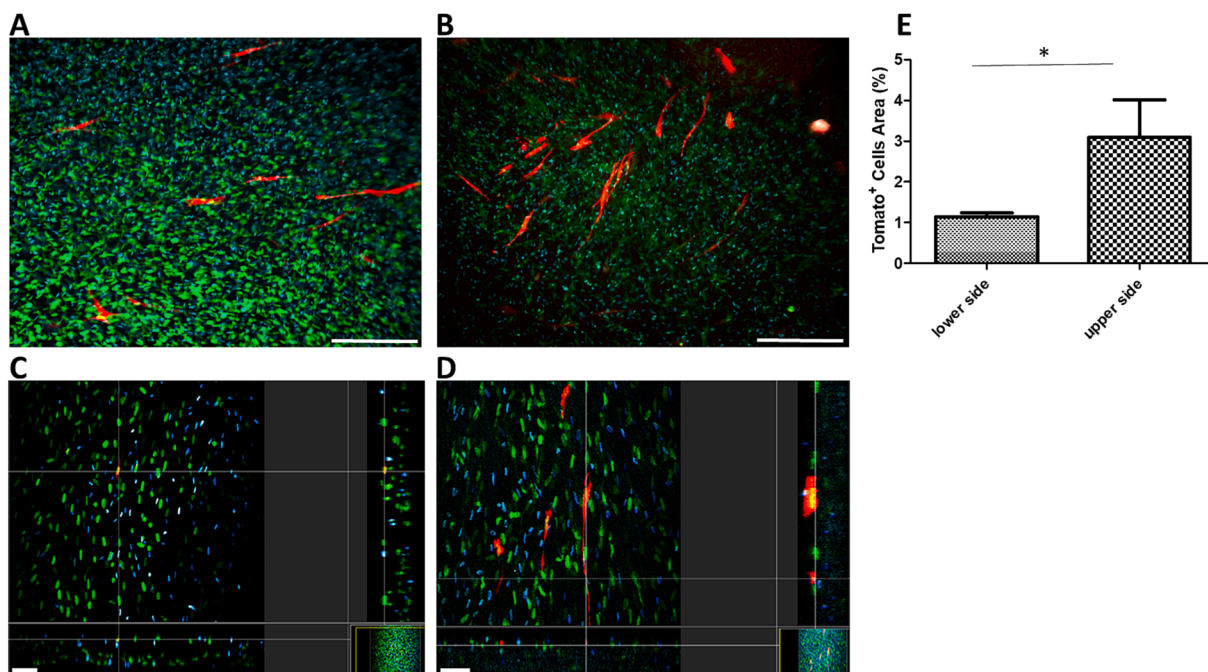


**Fig. 6.** Effect of cell gene electrotransfer on dermal cell-sheet depending on the localization of the plasmid DNA. Tomato expression in 3D cell sheets, submitted to 400 V/cm with 20 ms pulse duration, after plasmid deposition, observed by macroscopy (A-B) and multiphoton microscopy (B-C) 48 h after gene transfection on bottom (A-C) or upper side (B-D). A and B- Representative micrograph of Tomato expression in selected central zones of 3D dermal sheets, with labelled viable cells (syto16- green) and dead cells (Hoechst 33258-blue). Scale bar: 0,5 mm. C and D- Biphoton micrographs with orthogonal view showing Tomato positive cells (red), the localisation of viable cells (Syto-16) in green color and dead cells (Hoechst 33258) in blue color, in the dermal sheet 48 h after electroporation. Scale bar: 50  $\mu$ m. E- Quantification of Tomato-positive area in percentage (%) corresponding to the surface of the fluorescent electrotransfected cells relative to the total surface observed on the macrofluoro image of the dermal sheet. Unpaired *t*-test \*  $p < 0.05$  (N = 2; n = 6). (For interpretation of the references to color in this figure legend, the reader is referred to the web version of this article.)

high, they can cause tissue damage. Nevertheless, studies performed with monopolar pulses without the concomitant application of heat [38] and together with heating pre-treatment to 43–45 °C, both *in vitro* [39] and *in vivo* [40], indicated enhanced gene expression in HaCaT cells or in guinea pigs, respectively, where the skin was heated either with an IR laser or the Moor Skin heater, to enhance gene electrotransfer following plasmid intradermal injections [40]. Efficient heating appreciably facilitated gene electrotransfer in dermal and muscle cells in lowering required applied voltage, number of pulses and in allowing gene expression to deeper layers of the skin [40]. In addition, moderate heat-assisted gene electrotransfer approach could result in maintaining high expression for up to two weeks after a single delivery. This approach was suggested for protein replacement therapy and for cutaneous delivery of a plasmid encoding Hepatitis B surface antigen, which could be used as a DNA vaccine against Hepatitis B virus [41,42].

We thus also proceeded with local temperature measurement, to assess if temperature increase might have occurred in our experimental setting, and are explained in the following text.

### 3.5. Effect of electric pulses parameters on temperature increase

To determine if the loss of viability could be due to a large thermal increment, or if a small thermal increment could occur and thus alter the collagen structure in cell sheets, we measured the maximal temperature increase in the pulsing buffer during pulsation with a fiber optic temperature probe. Fig. 7 shows the temperature increase during pulse application, showing only a maximum of 2 °C increase for the condition 800 V/cm – 20 ms. The cell viability and collagen structure could therefore not be affected by the temperature increase occurring during the application of electric pulses.

Nevertheless, collagen destructure induced with a mild thermal treatment, or dermal sheet pre-treatment with hyaluronidase could be a promising alternative to treat the dermal sheet or more broadly, the skin, as it had already been shown, with the aim to improve the delivery of intramuscular gene electrotransfer-based protocols in mouse [43].

And finally, the potential explanation for the lack of efficiency in gene electrotransfer to tissues, could be the simple fact that multiple cell layers sterically hinder a homogenous distribution of plasmids around all cells, which together with the more or less tight meshwork of collagen fibres, prevent the penetration of plasmids to deep-layered cells, as we previously showed in a tumor cell spheroid model [44].

## 4. Conclusion

In combination with our previous work using contact parallel electrodes, the results presented herein indicate that when the electric field is perpendicular to the cell sheet, it has little if any effect on transfection efficiency. Only the cells present in the external layers of the cell sheet where the plasmid DNA was deposited could be modestly transfected. This could be due to the limited electrophoretic force and the presence of collagen fibres that prevent plasmid DNA diffusion (both laterally and vertically in the depth of the tissue). Importantly, increasing the electric field strength leads to a decrease in cell viability, yet increasing the pulse duration may help to increase plasmid DNA electrophoresis, as showed herein with 20 ms pulses.

While significant efforts and creativity will be required in the future to determine the optimal conditions that result in a high transfection yield through electroporation technology in complex, collagen rich tissues, electroporation remains promising for the delivery of nucleic acids into cells. While collagen indeed remains a hard nut to crack, decreasing the size of nucleic acids and focusing on molecules such as mRNA or siRNA, or locally denaturing the collagen barriers by heat or enzymes, could offer promising avenues to improve electrotransfer into the skin. Finally, engineered dermal tissue is a valid and relevant biological tool that complexifies *in vitro* models, and allows the investigation of the mechanisms of gene electrotransfer in human skin and thus represents a

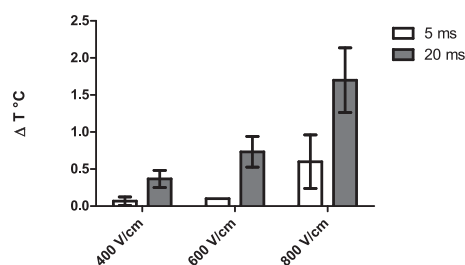


Fig. 7. Temperature increase quantification occurring during electropulsation. The graph represents the thermal increment due to the pulses for each experimental condition (400–600–800 V/cm) with 5 ms (white) and 20 ms (gray) pulse duration (N = 3 independent experiments).

reliable alternative to animal experiments.

### Funding statement

This research was funded by Fondation ARC [RF20170205456], LEROY Biotech “speedpores [238252] and “Plan France Relance” and the French national research agency (ANR) under the project CAR-BO2DERM (grant ANR-19-CE09-0007) and the project JOULMECT (grant ANR-23-CE18-0029-01).

### CRediT authorship contribution statement

**Géraldine Albérola:** Conceptualization, Data curation, Formal analysis, Methodology. **Elisabeth Bellard:** Data curation, Formal analysis, Methodology. **Jelena Kolosnjaj-Tabi:** Conceptualization, Formal analysis, Writing – review & editing. **Jorgan Guard:** Formal analysis. **Muriel Golzio:** Conceptualization, Formal analysis, Funding acquisition, Investigation, Supervision, Validation, Writing – original draft, Writing – review & editing. **Marie-Pierre Rols:** Conceptualization, Funding acquisition, Investigation, Methodology, Project administration, Supervision, Validation, Writing – original draft, Writing – review & editing.

### Declaration of competing interest

The authors declare that they have no known competing financial interests or personal relationships that could have appeared to influence the work reported in this paper.

### Data availability

Data will be made available on request.

### Acknowledgments

We thank the “Toulouse Réseau Imagerie” core IPBS facility (Genotoul, Toulouse, France).

### Appendix A. Supplementary data

Supplementary data to this article can be found online at <https://doi.org/10.1016/j.bioelechem.2024.108670>.

### References

- [1] K.S. Park, X. Sun, M.E. Aikins, J.J. Moon, Non-viral COVID-19 vaccine delivery systems, *Adv. Drug Deliv. Rev.* 169 (2021) 137–151.
- [2] N. Pardi, M.J. Hogan, F.W. Porter, D. Weissman, mRNA vaccines – a new era in vaccinology, *Nat. Rev. Drug Discov.* 17 (2018) 261–279.
- [3] J.P. Tasu, D. Tougeron, M.P. Rols, Irreversible electroporation and electrochemotherapy in oncology: State of the art, *Diagn. Interv. Imaging* 103 (2022) 499–509.

- [4] L.M. Mir, M. Belehradek, C. Domenge, S. Orłowski, B. Poddevin, J. Belehradek Jr., G. Schwaab, B. Luboinski, C. Paoletti, Electrochemotherapy, a new antitumor treatment: first clinical trial, *C. R. Acad. Sci. III* 313 (1991) 613–618.
- [5] R.V. Davalos, L.L. Mir, B. Rubinsky, Tissue ablation with irreversible electroporation, *Ann. Biomed. Eng.* 33 (2005) 223–231.
- [6] E. Neumann, M. Schaefer-Ridder, Y. Wang, P.H. Hofschneider, Gene transfer into mouse lymphoma cells by electroporation in high electric fields, *EMBO J.* 1 (1982) 841–845.
- [7] M. Golzio, J. Teissie, M.P. Rols, Direct visualization at the single-cell level of electrically mediated gene delivery, *Proc. Natl. Acad. Sci. U. S. A.* 99 (2002) 1292–1297.
- [8] C. Rosazza, A. Buntz, T. Riess, D. Woll, A. Zumbusch, M.P. Rols, Intracellular tracking of single plasmid DNA-particles after delivery by electroporation, *Mol. Ther.* (2013).
- [9] C. Rosazza, S.H. Meglic, A. Zumbusch, M.P. Rols, D. Miklavcic, Gene electrotransfer: A mechanistic perspective, *Curr. Gene Ther.* 16 (2016) 98–129.
- [10] M.P. Rols, C. Delteil, M. Golzio, P. Dumond, S. Cros, J. Teissie, In vivo electrically mediated protein and gene transfer in murine melanoma, *Nat. Biotechnol.* 16 (1998) 168–171.
- [11] A.I. Daud, R.C. DeConti, S. Andrews, P. Urbas, A.I. Riker, V.K. Sondak, P. N. Munster, D.M. Sullivan, K.E. Ugen, J.L. Messina, R. Heller, Phase I trial of interleukin-12 plasmid electroporation in patients with metastatic melanoma, *J. Clin. Oncol.* 26 (2008) 5896–5903.
- [12] A.V. Titimirov, S. Sukharev, E. Kistanova, In vivo electroporation and stable transformation of skin cells of newborn mice by plasmid DNA, *Biochim. Biophys. Acta* 1088 (1991) 131–134.
- [13] J. Dermol-Cerne, E. Pirc, D. Miklavcic, Mechanistic view of skin electroporation - models and dosimetry for successful applications: an expert review, *Expert. Opin. Drug Del.* 17 (2020) 689–704.
- [14] B. Ferraro, Y.L. Cruz, D. Coppola, R. Heller, Intradermal delivery of plasmid VEGF (165) by electroporation promotes wound healing, *Mol. Ther.* 17 (2009) 651–657.
- [15] A. Brave, S. Nystrom, A.K. Roos, S.E. Applequist, Plasmid DNA vaccination using skin electroporation promotes poly-functional CD4 T-cell responses, *Immunol. Cell Biol.* 89 (2011) 492–496.
- [16] S. Mazeret, D. Sel, M. Golzio, G. Pucihar, Y. Tamzali, D. Miklavcic, J. Teissie, Non invasive contact electrodes for in vivo localized cutaneous electroporation and associated drug and nucleic acid delivery, *J. Control. Release* 134 (2009) 125–131.
- [17] R. Heller, Y. Cruz, L.C. Heller, R.A. Gilbert, M.J. Jaroszeski, Electrically mediated delivery of plasmid DNA to the skin, using a multielectrode array, *Hum. Gene Ther.* 21 (2010) 357–362.
- [18] L. Pasquet, S. Chabot, E. Bellard, B. Markelc, M.P. Rols, J.P. Reynes, G. Tiraby, F. Couillaud, J. Teissie, M. Golzio, Safe and efficient novel approach for non-invasive gene electrotransfer to skin, *Sci. Rep.* 8 (2018) 16833.
- [19] L. Pasquet, S. Chabot, E. Bellard, M.P. Rols, J. Teissie, M. Golzio, Noninvasive gene electrotransfer in skin, *Hum. Gene Ther. Method* 30 (2019) 17–22.
- [20] A. Paganin-Gioanni, E. Bellard, J.M. Escoffre, M.P. Rols, J. Teissie, M. Golzio, Direct visualization at the single-cell level of siRNA electrotransfer into cancer cells, *Proc. Natl. Acad. Sci. U. S. A.* 108 (2011) 10443–10447.
- [21] S. Chabot, J. Teissie, M. Golzio, Targeted electro-delivery of oligonucleotides for RNA interference: siRNA and anti-miR, *Adv. Drug Deliv. Rev.* 81 (2015) 161–168.
- [22] C. Faurie, E. Phez, M. Golzio, C. Vossen, J.C. Lesbordes, C. Delteil, J. Teissie, M. P. Rols, Effect of electric field vectoriality on electrically mediated gene delivery in mammalian cells, *Biochim. Biophys. Acta* 1665 (2004) 92–100.
- [23] C. Faurie, M. Golzio, P. Moller, J. Teissie, M.P. Rols, Cell and animal imaging of electrically mediated gene transfer, *DNA Cell Biol.* 22 (2003) 777–783.
- [24] S.H. Meglic, M. Pavlin, The impact of impaired DNA mobility on gene electrotransfer efficiency: analysis in 3D model, *Biomed. Eng. Online* 20 (2021).
- [25] K.A. Athanasiou, R. Eswaramoorthy, P. Hadidi, J.C. Hu, Self-organization and the self-assembling process in tissue engineering, *Annu. Rev. Biomed. Eng.* 15 (2013) 115–136.
- [26] L. Gibot, T. Galbraith, J. Huot, F.A. Auger, Development of a tridimensional microvascularized human skin substitute to study melanoma biology, *Clin. Exp. Metastasis* 30 (2013) 83–90.
- [27] M. Madi, M.P. Rols, L. Gibot, Efficient in vitro electropermeabilization of reconstructed human dermal tissue, *J. Membr. Biol.* 248 (2015) 903–908.
- [28] M. Madi, M.P. Rols, L. Gibot, Gene electrotransfer in 3D reconstructed human dermal tissue, *Curr. Gene Ther.* 16 (2016) 75–82.
- [29] F. Pillet, L. Gibot, M. Madi, M.P. Rols, E. Dague, Importance of endogenous extracellular matrix in biomechanical properties of human skin model, *Biofabrication* 9 (2017).
- [30] B. Pintado, J. de la Fuente, E.R. Roldan, Permeability of boar and bull spermatozoa to the nucleic acid stains propidium iodide or Hoechst 33258, or to eosin: accuracy in the assessment of cell viability, *J. Reprod. Fertil.* 118 (2000) 145–152.
- [31] J. Simon, B. Jouanmiquet, M.P. Rols, E. Flahaut, M. Golzio, Transdermal delivery of macromolecules using two-in-one nanocomposite device for skin electroporation, *Pharmaceutics* 13 (2021).
- [32] M.P. Rols, J. Teissie, Electropermeabilization of mammalian cells. Quantitative analysis of the phenomenon, *Biophys. J.* 58 (1990) 1089–1098.
- [33] M. Golzio, J. Teissie, M.P. Rols, Cell synchronization effect on mammalian cell permeabilization and gene delivery by electric field, *BBA-Biomembranes* 1563 (2002) 23–28.
- [34] H.Q. Bai, G.M.S. Lester, L.C. Petishnok, D.A. Dean, Cytoplasmic transport and nuclear import of plasmid DNA, *Biosci. Rep.* 37 (2017).
- [35] D.A. Zaharoff, R.C. Barr, C.Y. Li, F. Yuan, Electromobility of plasmid DNA in tumor tissues during electric field-mediated gene delivery, *Gene Ther.* 9 (2002) 1286–1290.
- [36] S. Xu, H. Xu, W. Wang, S. Li, H. Li, T. Li, W. Zhang, X. Yu, L. Liu, The role of collagen in cancer: from bench to bedside, *J. Transl. Med.* 17 (2019) 1–22.
- [37] J. Kolosnjaj-Tabi, R. Di Corato, L. Lartigue, I. Marangon, P. Guardia, A.K. Silva, N. Luciani, O. Clement, P. Flaud, J.V. Singh, Heat-generating iron oxide nanocubes: Subtle “deconstructors” of the tumoral microenvironment, *ACS Nano* 8 (2014) 4268–4283.
- [38] A.A. Bulysheva, S. Arpag-McIntosh, C. Lundberg, M.P. Francis, R. Heller, Monopolar electrotransfer enhances gene delivery to a beating heart, *Mol. Ther.* 27 (2019) 182.
- [39] A. Donate, N. Burcus, K. Schoenbach, R. Heller, Application of increased temperature from an exogenous source to enhance gene electrotransfer, *Bioelectrochemistry* 103 (2015) 120–123.
- [40] A. Bulysheva, J. Hornef, C. Edelblute, C. Jiang, K. Schoenbach, C. Lundberg, M. A. Malik, R. Heller, Coalesced thermal and electrotransfer mediated delivery of plasmid DNA to the skin, *Bioelectrochemistry* 125 (2019) 127–133.
- [41] C. Edelblute, C. Mangiamela, R. Heller, Moderate heat-assisted gene electrotransfer as a potential delivery approach for protein replacement therapy through the skin, *Pharmaceutics* 13 (2021).
- [42] C. Edelblute, C. Mangiamela, R. Heller, Moderate heat-assisted gene electrotransfer for cutaneous delivery of a DNA vaccine against hepatitis B virus, *Hum. Gene Ther.* 32 (2021) 1360–1369.
- [43] M. De Robertis, L. Pasquet, L. Loiacono, E. Bellard, L. Messina, S. Vaccaro, R. Di Pasquale, V.M. Fazio, M.P. Rols, J. Teissie, M. Golzio, E. Signori, In vivo evaluation of a new recombinant hyaluronidase to improve gene electro-transfer protocols for DNA-based drug delivery against cancer, *Cancers* 10 (2018).
- [44] A. de Caro, E. Bellard, J. Kolosnjaj-Tabi, M. Golzio, M.-P. Rols, Gene electrotransfer efficiency in 2D and 3D cancer cell models using different electroporation protocols: A comparative study, *Pharmaceutics* 15 (2023) 1004.